# Graphical abstract:



Proliferating
Neural Progenitor Cells

PROX1 positive
neurons

iPSC

Yu at al.
Stem Cell Reports (2014)

Nestin
Sox2
nuclei

B-III-tubulin
PROX1

4-6w

SB-CAG-GCaMP6f    Fluo4AM
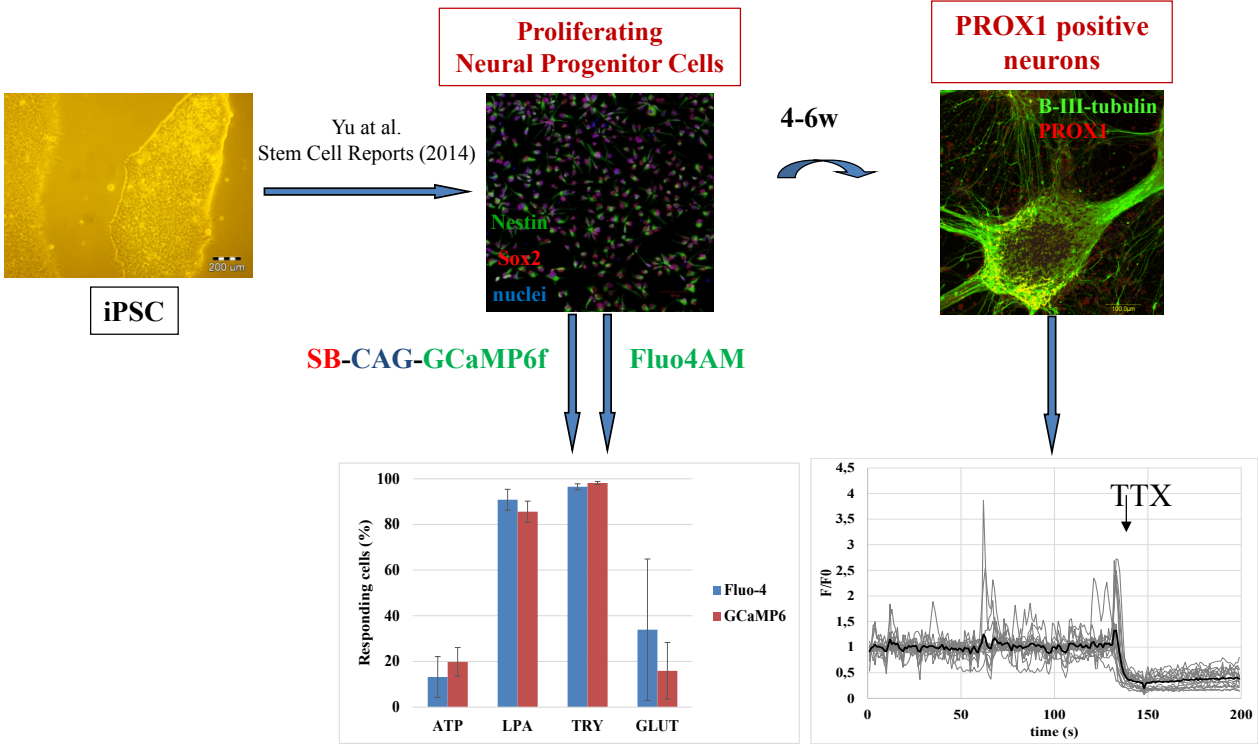
# Characterization of calcium signals in human induced pluripotent stem cell-derived dentate gyrus neuronal progenitors and mature neurons, stably expressing an advanced calcium indicator protein

Gergő Vőfély[a], Tünde Berecz[a], Eszter Szabó[a], Kornélia Szebényi[a], Edit Hathy[b], Tamás I. Orbán[a], Balázs Sarkadi[a,e], László Homolya[a], Maria C. Marchetto[c], János M. Réthelyi[b,d*], Ágota Apáti[a*]

[a]*Institute of Enzymology, Research Centre for Natural Sciences, Budapest, Hungary;*
[b]*MTA-SE NAP-B, Molecular Psychiatry and in vitro Disease Modelling Research Group, National Brain Research Project, Hungarian Academy of Sciences and Semmelweis University, Budapest, Hungary;*
[c]*Laboratory of Genetics, Salk Institute for Biological Studies, La Jolla, CA, United States;*
[d]*Department of Psychiatry and Psychotherapy, Semmelweis University, Budapest, Hungary*
[e]*Department of Biophysics and Radiation Biology, Semmelweis University, Budapest, Hungary.*

**\* Corresponding authors:**

**János M. Réthelyi**

Department of Psychiatry and Psychotherapy, Semmelweis University,

1083 Budapest, Balassa utca 6. Budapest, Hungary

Tel/Fax: +3612100336

Email: rethelyi.janos@med.semmelweis-univ.hu

**Ágota Apáti**

Institute of Enzymology, Research Centre for Natural Sciences

1117 Magyar tudósok körútja 2. Budapest, Hungary

Tel/Fax: +3613826607

Email: apati.agota@ttk.mta.hu/ apati@biomembrane.hu

**Abstract**

Pluripotent stem cell derived human neuronal progenitor cells (hPSC-NPCs) and their mature neuronal cell culture derivatives may efficiently be used for central nervous system (CNS) drug screening, including the investigation of ligand-induced calcium signalization. We have established hippocampal NPC cultures derived from human induced PSCs, which were previously generated by non-integrating Sendai virus reprogramming. Using established protocols these NPCs were differentiated into hippocampal dentate gyrus neurons. In order to study calcium signaling without the need of dye loading, we have stably expressed an advanced calcium indicator protein (GCaMP6fast) in the NPCs using the *Sleeping Beauty* transposon system. We observed no significant effects of the long-term GCaMP6 expression on NPC morphology, gene expression pattern or neural differentiation capacity. In order to compare the functional properties of GCaMP6-expressing neural cells and the corresponding parental cells loaded with calcium indicator dye Fluo-4, a detailed characterization of calcium signals was performed. We found that the calcium signals induced by ATP, glutamate, LPA, or proteases - were similar in these two systems. Moreover, the presence of the calcium indicator protein allowed for a sensitive, repeatable detection of changes in calcium signaling during the process of neurogenesis and neuronal maturation.

**Key words**

human iPSC; neuronal differentiation; hippocampus; dentate gyrus; calcium-imaging; GCaMP6

**Abbreviations**

hPSC: human pluripotent stem cell, hiPSC: human induced pluripotent stem cell, NPC: neuronal progenitor cell, hPSC-NPC: human pluripotent stem cell derived neuronal progenitor cell, EB: embryoid body, CNS: central nervous system, DG: dentate gyrus, GECI: genetically engineered calcium indicator, MEF: mouse embryonic fibroblast, PROX1: Prospero homeobox 1, DKK1: Dickkopf-related protein 1, FGF2: fibroblast growth factor 2, BDNF: brain-derived nerve factor, MAP2: microtubule-associated protein 2, CALB1: Calbindin 1, PAX6: Paired box 6, SOX2: SRY-box 2, P0: RPLP0 (Ribosomal Protein Lateral Stalk Subunit P0), GPC receptor: G protein-coupled receptor, DPBS: Dulbecco's modified PBS, HBSS: Hanks' balanced salt solution, DAPI: 4', 6-diamidino-2-phenylindole, AA: ascorbic

acid, LPA: lysophosphatidic acid, EGTA: ethylene glycol tetraacetic acid, TTX: tetrodotoxin ,
ICC: immunocytochemistry, GRIA1: glutamate ionotropic receptor AMPA type subunit 1

## 1. Introduction

Human pluripotent stem cells (hPSCs) can give rise *in vitro* to all cell types of the human body, including functional neurons (Shi, Y. et al., 2012; Nicholas, C. R. et al., 2013). This model system provides new possibilities to investigate the molecular disease pathways underlying neuropsychiatric disorders and allows generating tools for drug screening applications.

The dentate gyrus (DG) and the olfactory bulb are the two known regions of the rodent brain where neurogenesis persists into adulthood, while in the human brain this has only been shown consistently in the DG (Eriksson, P. S. et al., 1998). New neurons generated in the DG are essential for learning, pattern separation, and spatial memory formation (Zhao, C. et al., 2008). And alterations of hippocampal neurogenesis have been implicated in several disease conditions, including epileptic seizures (Jessberger, S. et al., 2007), Alzheimer's disease (Tatebayashi, Y. et al., 2003), cognitive defects characteristic of depression (Sahay, A. and Hen, R., 2008; Mateus-Pinheiro, A. et al., 2013) and schizophrenia (Reif, A. et al., 2006; Tamminga, C. A. et al., 2010; Walton, N. M. et al., 2012; Hagihara, H. et al., 2013; Shin, R. et al., 2013). Since animal models are often inefficient in recapitulating human CNS disorders, the generation of proper human cell-based systems has been proposed for both disease-modelling and drug screening purposes.

Neurons differentiated from hPSCs using various protocols, i.e. specific morphogenic patterning cues, show characteristics of multiple neuronal subtypes (Kozubenko, N. et al., 2010; Kim, Y. S. and Park, C. H., 2011; Li, W. et al., 2011); moreover, this heterogeneity can already be monitored at the progenitor state (Forostyak, O. et al., 2013; Viero, C. et al., 2014). Most recently Yu et al. (Yu, D. X. et al., 2014) have developed a new protocol to generate hPSC-derived neural progenitor cells (NPCs) that preferentially differentiate into population enriched in hippocampal DG granule cells expressing Prospero Homeobox 1 (PROX1), thus recapitulating adult neurogenesis *in vitro*. Using transplantation experiments the authors demonstrated that after engraftment into the developing DG of P10 mice, the NPCs differentiated into electrophysiologically active PROX1-expressing neurons. Moreover, it was shown that directed differentiation to hippocampal granule neurons could reveal disease-related phenotypes in the human induced pluripotent stem cell (hiPSC) model of schizophrenia (Yu, D. X. et al., 2014) and bipolar disorder (Mertens, J. et al., 2015).

Calcium ions, as ubiquitous intracellular messengers, play a fundamental role in numerous cellular processes, including proliferation, differentiation, and excitability. The measurement of neuronal calcium signaling has recently become an important tool to study calcium channel activity, intracellular calcium release, as well as calcium-dependent neurotransmitter release in *in vitro* cultured NPCs and neurons (Malmersjo, S. et al., 2010; Chen, T. W. et al., 2013; Forostyak, O. et al., 2013; Malmersjo, S. et al., 2013; Smedler, E. et al., 2014). It has been suggested (Forostyak, O. et al., 2013) that calcium signals are highly variable during long-term culturing of NPCs, and ligand-induced calcium transients may be predictive of their ability to generate mature neurons.

The methods applicable for studying both short and long-term calcium responses are mostly based on the use of fluorescent calcium indicator dyes or calcium-sensitive fluorescent proteins. The use of the fluorescent calcium sensitive dyes, e.g. Fura-2, Fluo-4, or Xrod, has numerous drawbacks, including an inhomogeneous cellular distribution of the dye, liberation of toxic metabolites from the cell-permeable compounds, as well as photo-bleaching of the indicator (for details see (Apati, A. et al., 2012; Apati, A. et al., 2013)). These problems are especially relevant in highly sensitive, long-term cultured, and selectively differentiated cell types, such as neural precursors and neurons.

Genetically engineered calcium indicator (GECI) proteins, including the members of the GCaMP protein family, may serve as important tools for monitoring cellular calcium signals and provide the advantage of long-term repeated studies in cell cultures. The recently developed members of this GCaMP protein family, especially GCaMP6 has been documented to allow for highly sensitive and rapid cellular calcium signal measurements, relevant in excitable cells (Chen, T. W. et al., 2013). However, for a successful application of these potentially calcium-buffering fluorescent indicators in a properly conserved cellular milieu, their unknown cellular and developmental effects in human neuronal cell types are needed to be examined in detail.

In the present work we used the previously published differentiation protocol of Yu et al. (Yu, D. X. et al., 2014), and established hPSC-derived NPC cultures for the generation of PROX1-expressing hippocampal granule cells. In order to carry out calcium imaging studies we have also generated NPCs that stably express the GCaMP6fast calcium indicator protein. We have characterized these NPCs as well as the NPC-derived mature neurons in terms of morphology and function. Calcium signals measured in GCaMP6-expressing NPCs and their PROX1-expressing progenies were compared to that seen in Fluo-4 loaded parental NPCs and differentiated neurons, respectively. In summary, we demonstrated cell- and development-

specific calcium responses *in vitro,* and confirmed that GCaMP6-expressing cells are amenable for long-term calcium imaging studies.

2. **Methods**

*2.1 Cell culturing and differentiation*

A human iPSC line generated from fibroblasts of a healthy male individual by Sendai virus (Thermo Fisher Scientific, Massachusetts, USA) based reprogramming was maintained on mitomycin-C (Sigma, Missouri, USA) treated mouse embryonic fibroblast feeder cells (Millipore, Billerica, USA). The pluripotent state and spontaneous differentiation capacity of iPSCs were tested by real-time quantitative PCR and ICC as described previously (Erdei, Z. et al., 2014) (see first panel of Fig 1 A and suppl. Fig 1). Neural progenitor cells (NPCs) were differentiated as described previously (Yu, D. X. et al., 2014). Briefly, before starting differentiation, iPSC cells were transferred to Matrigel (Corning, New York, USA) coated plates in mTeSR medium (Stemcell Technologies, Vancouver, Canada) and were cultured to high density. On day 1 the cells were detached with collagenase (Thermo Fisher Scientific, Massachusetts, USA) and transferred to ultra-low attachment plates (Nalgene Nunc International, New York, USA). After embryoid body (EB) formation on day 3, the medium was changed to DMEM/F-12, GlutaMAX™ (Thermo Fisher Scientific, Massachusetts, USA) medium supplemented with N2/B27 (Thermo Fisher Scientific, Massachusetts, USA) and anticaudalizing agents (Noggin (Thermo Fisher Scientific, Massachusetts, USA), DKK1 (PeproTech, New Jersey, USA), Cyclopamine (Merck, Darmstadt, Germany), and SB431542 (Sigma, Missouri, USA)). The treatment was repeated every other day. On day 20 the EBs were moved to a poly-ornithine (Sigma, Missouri, USA)/laminin (Thermo Fisher Scientific, Massachusetts, USA) coated plate to support further differentiation in adherent conditions. On Day 27 or later, manually picked rosettes were dissociated by Accutase (Thermo Fisher Scientific, Massachusetts, USA) and re-seeded onto a new poly-ornithine/laminin coated plate in DMEM/F-12, GlutaMAX™ N2/B27 medium containing FGF2 (Thermo Fisher Scientific, Massachusetts, USA) and laminin. The attached neural progenitor cells (NPCs) showed uniform morphology after 5 passages. The NPCs between passage p5 and p15 were used for the experiments. For calcium imaging studies the parental and GCaMP6-expressing NPCs were further differentiated as described previously (Yu, D. X. et al., 2014). NPCs were seeded onto poly-ornithine/laminin coated, in eight-well Nunc Lab-Tek II Chambered Coverglass

(Nalgene Nunc International, New York, USA) with $1.5 \times 10^3$ density in N2/B27 medium supplemented with ascorbic acid (Sigma, Missouri, USA), BDNF (PeproTech, New Jersey, USA), cAMP (Sigma, Missouri, USA), Laminin and Wnt3A (Research and Diagnostic Systems Inc, Minnesota, USA). After 3 weeks Wnt3A was omitted from the media. The medium was changed every other day. The $Ca^{2+}$ signaling experiments were performed between 4 and 5 weeks of neural differentiation. Immunocytochemistry and qPCR measurements were performed after calcium imaging from selected wells of differentiated neural cultures.

## 2.2 Generation of GCaMP expressing NPCs

The NPCs were propagated as described previously (Yu, D. X. et al., 2014) and transfected at passage number p6. The plasmid used in this project contained the cDNA of GCaMP6fast, a genetically encoded calcium sensor, developed for imaging neural activity (Chen, T. W. et al., 2013). The original pGP-CMV-GCaMP6fast plasmid was purchased from Addgene (plasmid # 40755, deposited by Douglas Kim). The GCaMP6 coding sequence was cloned into a *Sleeping Beauty* transposon plasmid, downstream to a CAG promoter variant which was previously reported to provide a stable transgene expression in human embryonic stem cells and their differentiated derivatives (Orban, T. I. et al., 2009). Transposon-based gene delivery was performed using the SB100x hyperactive transposase OT (Mates, L. et al., 2009), followed by selection of the transgene expressing cells with 1.6 µg/ml puromycin for 48 hours, as the transposon cassette included a second transcription unit expressing a puromycin resistance gene (suppl. Fig 2). After one passage the selection procedure was repeated. The copy numbers of GCaMP6-expressing NPCs were determined using qPCR as described previously (Kolacsek, O. et al., 2011), yielding an average copy numbers of 14 and 8 in the NPC cell cultures used for studies.

## 2.3 Immunocytochemical staining

For immunofluorescence staining of NPCs and NPC-derived neurons, parental and GCaMP6-expressing NPCs were seeded onto poly-ornithine/laminin coated, eight-well chambers, and differentiated into DG neurons for 5 weeks as described above. The cells were fixed with 4% paraformaldehyde (Thermo Fisher Scientific, Waltham, Massachusetts, USA) in Dulbecco's modified PBS (DPBS) (Sigma, Missouri, USA) for 15 min at room temperature. Following washing with DPBS, the samples were blocked for 1h at room

temperature in DPBS containing 2 mg/ml bovine serum albumin (Sigma, Missouri, USA), 1% fish gelatin (Sigma, Missouri, USA), 5% goat serum (Sigma, Missouri, USA) and 0.1% Triton-X 100 (Sigma, Missouri, USA). The samples were then incubated for 1h at room temperature with the following antibodies: anti-AFP (monoclonal/mouse, 1:500 dilution; WH0000174M1, Sigma/Merck, Darmstadt, Germany), anti-B III tubulin (monoclonal/mouse, 1:2000 dilution; MAB1195, R&D Systems, Minneapolis, USA), anti-SMA (monoclonal/mouse, 1:100 dilution; ab7817, Abcam, Cambridge, UK), anti-SOX2 (monoclonal/mouse, 1:20 dilution; MAB2018, R&D Systems, Minneapolis, USA), anti-Nestin (polyclonal/rabbit, 1:250 dilution; ab92391, Abcam, Cambridge, UK) or for overnight at 4°C with the following antibodies: anti-PROX1 (polyclonal/rabbit, 1:500 dilution; ab101851, Abcam, Cambridge, UK), anti- CALB1 (monoclonal/mouse, 1:1000 dilution; Swant #300, Swant Inc., Switzerland), anti-MAP2 (monoclonal/mouse, 1:500 dilution; M1406, Sigma/Merck, Darmstadt, Germany or polyclonal/rabbit, 1:1000 dilution; ab5622, Millipore, Massachusetts, USA). After washing with DPBS, the cells were incubated for 1h at room temperature with appropriate secondary antibodies; Alexa Fluor 633-conjugated goat anti-mouse IgG or Alexa Fluor 547-conjugated goat anti-rabbit IgG (Thermo Fisher Scientific, Massachusetts, USA). The nuclei were counterstained with DAPI (Thermo Fisher Scientific, Massachusetts, USA). The stained samples were examined by an Olympus FV500-IX confocal laser scanning microscope. Fluorescence images were analyzed with the FluoViewTiempo (v4.3, Olympus, http://www.olympusmicro.com) software. In the confocal images pseudo-color coding was used for better visualization.

*2.4 Gene expression analysis*

Total RNA was isolated from iPSCs, NPCs and NPCs-derived neural cells using TRIzol™ reagent following the manufacturer's instructions (Thermo Fisher Scientific, Massachusetts, USA). cDNA samples were prepared from 0.2 µg total RNA using the Promega Reverse Transcription System Kit (Promega, Wisconsin, USA) as specified by the manufacturer. For real-time quantitative PCR the following Pre-Developed TaqMan® assays were purchased from Thermo Fisher Scientific, Massachusetts, USA: Oct4, NANOG as undifferentiated stem cell markers; T-Brachyury, Pax6 and AFP as mesoderm, ectoderm and endoderm markers respectively; SOX2, NESTIN and Glutamate Receptor (GRIA1) as markers of NPC state, as well as PAX6, NeuroD1, and PROX1 as neural differentiation specific markers; P0 ribosomal protein as endogenous control for quantification. RT-PCR analyses were carried out using the StepOnePlus™ Real-Time PCR System (Thermo Fisher

Scientific, Massachusetts, USA), according to the manufacturer's instructions. The changes in mRNA levels between the examined and control cells were determined by the $2^{-\Delta Ct}$ method using RPLP0 (P0) as endogenous control gene. Relative mRNA levels were presented as mean values ± S.D. of 3 independent experiments.

*2.5 Calcium signal measurements*

Before the calcium measurements, parental and GCaMP6fast expressing NPCs were seeded for two days onto eight-well chambers previously coated with poly-ornithine/laminin. For Fluo-4 studies, the parental NPCs cells subjected to 1.0 µM Fluo-4 AM (Thermo Fisher Scientific, Massachusetts, USA) in a serum free culture medium for 30 min at 37°C. Extracellular Fluo-4 AM was removed by changing the medium to Hanks' balanced salt solution (Thermo Fisher Scientific, Massachusetts, USA), supplemented with 20 mM Hepes (pH=7.4) (Thermo Fisher Scientific, Massachusetts, USA) and 0.9 mM MgCl2 (Sigma, Missouri, USA) (HBSS) - all the actual measurements were performed in HBSS. The ligand concentrations were chosen according to literature: ATP (100 µM) and suramin (600 µM ) (Thermo Fisher Scientific, Massachusetts, USA), trypsin (2.5 µg/ml) (Thermo Fisher Scientific, Massachusetts, USA), trypsin inhibitor from soybean (100 µg/ml) (Sigma, Missouri, USA), lysophosphatidic acid (LPA,10 µM) (Sigma, Missouri, USA), KCl (50 mM) (Sigma, Missouri, USA), glutamate (50 µM) (Sigma, Missouri, USA), ionomycin (5 µM) (Thermo Fisher Scientific, Massachusetts, USA). For calibration procedures to achieve low external calcium, EGTA (Sigma, Missouri, USA) was used in 5-fold excess of calcium concentration in the medium. All experiments were performed at room temperature.

Calcium signal measurements were carried out by acquisition of time lapse sequences of cellular fluorescence images with the FluoViewTiempo (v4.3, Olympus, http://www.olympusmicro.com) software as described earlier (Pentek, A. et al., 2016). Fluorescence images were acquired between 505 and 525 nm at 488 nm excitation. Image analysis was carried out with the same software. The fluorescence data were normalized to a calibrated range of cellular calcium levels ($F_{max}$–$F_{min}$). Data are means (±SD) of all the individual cells (typically 200-300 cells/ for each conditions) at least from 3 parallel experiments.

## 3. Results

*3.1 GCaMP6-expressing human NPCs retain basic characteristics of parental cells and can be differentiated into mature neurons.*

Consistent with earlier studies (Forostyak, O. et al., 2013; Viero, C. et al., 2014), our results indicate that the characteristics of iPSC-derived hippocampal NPCs, including morphology as well as proliferation and differentiation capacity, significantly depend on the duration of culturing time. We found that hippocampal NPCs became homogenous at passage 5 after mechanical separation of the rosettes, and could be used for differentiation experiments up to passages 15-20.

By using the proliferating NPCs, we transfected the cDNA constructs of GCaMP6 into these cells at passage number p6 using the *Sleeping Beauty* transposon-based vector containing a puromycin selection marker (see Methods). The transfection efficiency was above 30% (data not shown) 48 hours after transfection based on the percentage of green fluorescent cells. After the enrichment of the stable transgene positive cells by repeated puromycin selection, cells with green fluorescence were further propagated in puromycin-free culture media, and neural differentiation potential was monitored.

The parental and GCaMP6-expressing NPCs were differentiated using BDNF, cAMP, Wnt3A, and ascorbic acid for enrichment of hippocampal dentate gyrus (DG) granule neurons. The stable, still proliferating hPSC-derived hippocampal NPC cultures and differentiated hippocampal dentate gyrus (DG) granule neurons were characterized by mRNA expression profiling of specific markers and immunofluorescence staining.

As shown in Figure 1 A, assessment of mRNA expression levels of the pluripotency markers in both parental and GCaMP6-expressing NPCs during iPSC differentiation to NPCs and further differentiation of NPCs to DG neurons demonstrated that Oct 3/4, and Nanog significantly decreased, SOX2 did not significantly alter, while the neural progenitor marker Nestin slightly increased in NPCs and decreased in neural cells. mRNA levels of Pax6, NeuroD1 and PROX1, markers characteristic of dentate gyrus differentiation, were upregulated in mature neurons (for p values of significance see Supplementary Figure 3).

Figure 1 B -F demonstrate the morphology and immunocytochemical features of parental, and the GCaMP6-expressing NPCs (B and C), as well as the differentiated neurons thereof (D-F). We found that both the parental and GCaMP6-expressing NPCs showed positive staining for SOX2 and Nestin (C); the morphology of the transfected cells was not altered by

the gene delivery or GCaMP6 expression (B and C). NPC-derived DG neurons showed intensive staining for MAP2, highlighting their neuronal morphology (Fig 1 D), and proved to have PROX1 and CALB1 protein expression, markers of dentate gyrus granule cells (Figure 1 E and F). Cell counts for PROX1-positivity yielded 52.9% (SD=7.6, n=11 images) vs. 55.4% (SD=12.7, n=11 images) in the parental and GCAMP6-expressing mature neuronal cultures, respectively (t-test, p=0.6163). All morphological, immunocytochemical and mRNA expression features of the GCaMP6-expressing NPCs and neurons were preserved.

*3.2 Ligand-induced calcium signalization in hippocampal NPCs*

We performed a detailed characterization of the spontaneous and ligand-induced calcium signals in the NPC cultures. In order to explore the potential changes during cell culturing, we used various passage numbers of the NPC cultures. In all experiments, we compared the calcium signals obtained after Fluo-4 loading of the parental cells, and in parallel, the calcium transients observed in the GCaMP6-expressing cell cultures.

Figure 2 A and B show typical calcium imaging experiments in NPCs, either loaded with Fluo-4 (Panel A), or expressing the GCaMP6 indicator protein (Panel B). As documented, the cells do not show significant spontaneous calcium transients, while after the addition of ATP, LPA, or trypsin, both the Fluo-4 loaded and the GCaMP6-expressing NPCs respond with marked calcium signals. A final calibration of the calcium response was performed in all cases. The maximal fluorescence signal was determined by the addition of ionomycin, and the background, calcium-independent fluorescence was measured by a subsequent addition of excess EGTA to the medium (see Methods).

The observed calcium signals reflect the activation of purinergic receptors by ATP, GPC receptor activation by LPA, and the activation of protease-sensitive receptors by trypsin, respectively. The signals evoked by ATP and trypsin were abolished by pre-treatment with specific inhibitors, suramin (a P2 purinergic receptor inhibitor, 600 µM) and trypsin inhibitor (100 µg/ml) respectively as documented in suppl. Fig 4. Based on numerous similar experiments, we found no significant differences between the Fluo-4 loaded or the GCaMP6-expressing cells in terms of either in the proportion of the responding cells (Figure 2C) or the magnitude of the responses (Figure 2D). The spontaneous calcium gradients in NPCs were rarely detectable, however calcium oscillation after ligand induction was noticeable (in nearly 20% of the Fluo-4-loaded cells ($n_{cells}$=181), and in 25% of the GCaMP6-expressing cells ($n_{cells}$=129)), as demonstrated by the representative curves in Figure 2 E and F. The number of

the NPCs responding to the specific neurotransmitter molecule, glutamate was highly variable, exhibiting between 20 to 80% responders with low signal intensity (Figure 2 C and D).We could not observe any dependence on passage number or confluency of the cultures. To checked whether variability in glutamate-induced calcium-responses depend on differences in gene expression levels between passage numbers, mRNA level of ionotropic receptor AMPA type subunit 1 (GRIA1) was measured. mRNA levels for GRIA1 showed no significant differences with passage number neither in GCAMP6-expressing nor wild type NPCs (suppl. Fig 5). As representative curves show (suppl. Figure 6), the intracellular calcium level increased slowly after addition of glutamate and remained at a new steady state level for minutes. Again, we could not find any significant difference between GCaMP6-expressing and Fluo-4 loaded NPCs.

NPCs, either loaded with Fluo-4 or expressing GCaMP6, reacted with very subtle response to an increased potassium level in the medium (see suppl. Figure 6). Only a few cells showed a calcium signal after the addition of 50 mM KCl. Although the number of responding cells increased slightly by passage number of the cultures, this still remained under 5%. These findings indicate that undifferentiated dentate gyrus NPCs do not respond with calcium transients to changes in the membrane potential (KCl), while increasing passages may induce a partial differentiation of the cultured NPCs.

*3.3 Human DG granule cells differentiated form parental and GCaMP6-expressing NPCs exhibit spontaneous calcium signal activity*

Next, to investigate calcium signal activity in mature, PROX1-expressing DG neurons derived from hippocampal NPCs, we carried out calcium-imaging experiments after 4-5 weeks of differentiation, as shown in Figures 3 and 4. A key feature of these neurons, either loaded with Fluo-4 or expressing GCaMP6, is the significant level of spontaneous calcium signaling activity (see Supplementary videos 1 and 2). The complex neuronal network formed under these conditions is well reflected by the rapid, partially coupled, spontaneous calcium transients observed in single neurons. It is important to emphasize that the fluorescence response rate of the highly sensitive GCaMP6 protein to changes of intracellular calcium concentration allows the following of rapid cellular calcium changes in individual cells, similarly to the Fluo-4 indicator.

We found that the differentiated DG neurons fully respond (practically 100%) with a large calcium signal to changes in the membrane potential elicited by the addition of KCl to the

medium, or to the addition of 50 µM glutamate (Figures 3 A and 3 B). We observed a trend for higher fluorescence signal intensity in GCaMP6-expressing neurons compared to their Fluo-4 loaded counterparts, however, this difference did not reach statistical significance (Supplementary Figures 7 A and B). Addition of 100 µM of tetrodotoxin (TTX), a voltage-gated sodium-channel blocker, abolished spontaneous calcium activity in both the GCaMP6-expressing and Fluo-4 loaded mature neurons (Figure 5). Sensitivity to TTX demonstrates that spontaneous calcium activity in these neuronal cultures is action potential dependent.

The spontaneous calcium signals and responses to neuromodulators under various culturing conditions are important characteristics of the iPSC-derived specific neuronal systems. A key advantage of using GCaMP6-expressing NPCs and differentiated neurons is the ability to perform long-term, continuous calcium signaling studies with the same cell preparations over time and after changing culture conditions. This feature is documented in Figure 4, by examining spontaneous calcium oscillations in individual cells of neuronal cultures. Panels A and B show the single cell calcium transients recorded in differentiated (after 4 weeks of differentiation) neuronal cultures either loaded with Fluo-4 (A) or expressing GCaMP6 (B). Panel C documents similar spontaneous calcium signals in the same GCaMP6-expressing cell culture as the one shown in Panel B, but cultured for a further 10 days. These data document that even a long-term expression of the GCaMP6 calcium indicator protein and repeated measures have no significant detrimental effect on the cultured neuronal cells.

## 4. Discussion

The physiological relevance of hPSC-derived NPCs and neurons, as well as that of their comparability to endogenous equivalents remain a subject of debate (Conti, L. and Cattaneo, E., 2010; Gage, F. H. and Temple, S., 2013; Suzuki, I. K. and Vanderhaeghen, P., 2015). Therefore, a better understanding of these models will be critical to control NPC differentiation and to make NPCs suitable for disease modelling and drug screening. Several methods have been established for the generation of human neurons (Elkabetz, Y. et al., 2008; Koch, P. et al., 2009; Kozubenko, N. et al., 2010); reviewed in (Conti, L. and Cattaneo, E., 2010; Mertens, J. et al., 2016), resulting in variable NPC cultures and differentiated neural cells with broad cellular heterogeneity. Therefore we have adopted a recently developed differentiation method for the generation of specific NPCs, providing disease-relevant subtype of neurons, namely DG granule cells (Yu, D. X. et al., 2014). Adult neurogenesis is less easily

studied in humans and may be fundamentally different compared to adult neurogenesis in the rodent brain (reviewed by (Ernst, A. and Frisen, J., 2015)), however iPSC-derived PROX1-expressing human in vitro neurons recapitulate the development of the dentate gyrus and in some aspects adult neurogenesis; therefore they could serve as a useful model for investigating psychiatric disorders.

The NPCs generated by this method showed homogenous morphology and unchanged differentiation capacity between passage numbers 5 and 15. Using immunostaining and qPCR assays (Fig 1), we found that the NPCs obtained by this method showed high levels of SOX2, Nestin and PAX6 expression, while the expression of NeuroD1 and PROX1 increased during differentiation. The 4 week old neurons were positive for MAP2, a mature neuronal marker (Yu, D. X. et al., 2014). We also found that the expression of pluripotency markers Oct4 and Nanog significantly decreased in NPCs and 4 week old neurons; however Nanog expression was higher in neurons than in NPCs. This may be the consequence of a 3 week long WNT3A treatment at the beginning of neural differentiation,  as WNT3A stimulation may induce the transcription of NANOG at least in cultured endothelial cells (Kohler, E. E. et al., 2011).

Forostyak et al. (Forostyak, O. et al., 2013) demonstrated the variability of calcium signals during long-term culturing of NPCs, obtained by a different, less specific, broader protocol. In order to investigate this type of variability, we have tested our NPCs between p8 and p15. In contrast to the aforementioned study, where ligand-based calcium-activity changed gradually between p6 and p10, we found that the calcium signals obtained after the addition of ATP, LPA, trypsin and KCl (regarding the number of responding cells and intensity of calcium signals) were not significantly dependent on the passage number. However consistent with previously published study (Forostyak, O. et al., 2013; Viero, C. et al., 2014), the calcium signals after the addition of glutamate showed high variability with regard to the number of responding cells, while the intensity of signals did not change significantly (Suppl. Figures 3 A and B). We observed some partially differentiated cells (less than 5%) during a prolonged culturing of NPCs. These cells showed neurite outgrowths and gave moderate calcium signals after the addition of KCl. Our results indicate that NPCs with broader differentiation capacity (Kozubenko, N. et al., 2010; Forostyak, O. et al., 2013) may be more variable in their calcium signaling properties than the NPCs with more restricted differentiation properties (Yu, D. X. et al., 2014).

For *in vitro* calcium measurement calcium sensitive dyes, such as Fluo-4/AM, Fura-2/AM or Oregon green 488 BAPTA-1 AM (OGB1-AM), are extensively used, while for *in vivo* experiments the use of genetically engineered calcium indicator (GECI) proteins is greatly

increasing (Rose, T. et al., 2014; Apati, A. et al., 2016; Dana, H. et al., 2016). In our previous study (Apati, A. et al., 2013), we compared the application of the calcium sensitive fluorescent dye, Fluo-4, and the GECI GCaMP2, for studying calcium signaling in human PSCs. Our results showed that the differentiation properties were fully preserved in the GCaMP2-expressing hPSC lines, and calcium imaging studies could be efficiently performed. However, the utility of GCaMP2 for studying calcium signaling in neural cell types is limited due to its kinetic properties, especially when spontaneous calcium spikes or lower intensity signals should be measured. Therefore, in the current study we have applied a new GCaMP variant (GCaMP6fast), which has been demonstrated to produce higher sensitivity than commonly used synthetic calcium dyes (e.g., OGB1), and detect individual action potentials *in vivo* in the mouse brain (Chen, T. W. et al., 2013; Dana, H. et al., 2014; Guo, Q. et al., 2015). The NPCs studied here were proved to be easily transfectable (in comparison with hPSCs) and the GCaMP6-expressing NPCs preserved their morphology and gene expression profiles. Moreover, the NPC-derived, GCaMP6-expressing neural cells formed expanded neural network with spontaneous calcium transients, similar to the Fluo-4-loaded cells. There were no significant differences between the GCaMP6-expressing and Fluo-4-loaded cells in ligand induced or spontaneous calcium signals regarding the number of responding cells and signal intensities.

Calcium-imaging has been shown to be a powerful method in hiPSC-based disease modeling studies. Specific alterations have been detected using this method in disease-associated neuronal cultures, including decreased calcium-activity and neuronal connectivity in Rett-syndrome and schizophrenia-derived neurons (Marchetto, M. C. et al., 2010; Yu, D. X. et al., 2014). Hyperexcitability in hiPSC-derived neuronal cultures of patients diagnosed with bipolar affective disorder has also been reported (Mertens, J. et al., 2015). We propose that the application of a GECI with favorable kinetic properties in neuronal cultures derived from either healthy or diseased individual represents a robust system for studying the phenomena of neuronal differentiation and regeneration, as well as emerging network properties. The cells expressing fast kinetic GECI are also amenable to high-throughput drug-screening. Previous studies, using specific marker analysis by immunocytochemistry or mRNA assays, examined the changes induced by various ligands and drug candidates at endpoints rather than the dynamic process of neuronal differentiation and functional maturation (Zhao, W. N. et al., 2012; Boissart, C. et al., 2013). However, future studies applying GCaMP6 expression in cultured human neurons could be carried out to test these effects. Another possible future application of this system is the investigation of the role of

calcium signalization in the processes of migration and proliferation in NPCs, and differentiation into neurons (for review see (Toth, A. B. et al., 2016)). For example one could track the emergence of spontaneous, rhythmic calcium activity after changing culture conditions and shifting NPCs from proliferation to differentiation. Also, GCaMP6-expressing NPCs could be grafted into murine or human *ex vivo* slice preparations to test the functional integration, spontaneous activity and potential regenerative properties of these hIPSC derived neuronal cells. Initial studies for transplantation experiments both in *ex vivo* and *in vivo* studies have shown promising results (Tabar, V. and Studer, L., 2014; Yu, D. X. et al., 2014; Daviaud, N. et al., 2015; Steinbeck, J. A. and Studer, L., 2015; Hiragi, T. et al., 2017).

## 5. Conclusions

In summary, the present study demonstrates that NPCs and neural networks can be efficiently studied in terms of calcium signaling properties by the stable expression of a new generation GECI, GCaMP6. By using this technique, calcium imaging can be performed without the need of potentially toxic dye -loading of cells before the experiments. Cultured GCaMP6-expressing NPCs and mature neurons allow repeated functional investigations for an extended time period and provide a new and efficient experimental system for pharmacological and toxicological studies in human neuronal cultures.

## 6. Competing Interests

The authors declare no competing financial interests.

## 7. Acknowledgements

## 8. References

Apati, A., Berecz, T.Sarkadi, B., 2016. Calcium signaling in human pluripotent stem cells. Cell calcium. 59, 117-23.

Apati, A., Paszty, K., Erdei, Z., Szebenyi, K., Homolya, L.Sarkadi, B., 2012. Calcium signaling in pluripotent stem cells. Molecular and cellular endocrinology. 353, 57-67.

Apati, A., Paszty, K., Hegedus, L., Kolacsek, O., Orban, T. I., Erdei, Z., Szebenyi, K., Pentek, A., Enyedi, A.Sarkadi, B., 2013. Characterization of calcium signals in human embryonic stem cells and in their differentiated offspring by a stably integrated calcium indicator protein. Cellular signalling. 25, 752-9.

Boissart, C., Poulet, A., Georges, P., Darville, H., Julita, E., Delorme, R., Bourgeron, T., Peschanski, M.Benchoua, A., 2013. Differentiation from human pluripotent stem cells of cortical neurons of the superficial layers amenable to psychiatric disease modeling and high-throughput drug screening. Transl Psychiatry. 3, e294.

Chen, T. W., Wardill, T. J., Sun, Y., Pulver, S. R., Renninger, S. L., Baohan, A., Schreiter, E. R., Kerr, R. A., Orger, M. B., Jayaraman, V., Looger, L. L., Svoboda, K.Kim, D. S., 2013. Ultrasensitive fluorescent proteins for imaging neuronal activity. Nature. 499, 295-300.

Conti, L. and Cattaneo, E., 2010. Neural stem cell systems: physiological players or in vitro entities? Nature reviews. Neuroscience. 11, 176-87.

Dana, H., Chen, T. W., Hu, A., Shields, B. C., Guo, C., Looger, L. L., Kim, D. S.Svoboda, K., 2014. Thy1-GCaMP6 transgenic mice for neuronal population imaging in vivo. PloS one. 9, e108697.

Dana, H., Mohar, B., Sun, Y., Narayan, S., Gordus, A., Hasseman, J. P., Tsegaye, G., Holt, G. T., Hu, A., Walpita, D., Patel, R., Macklin, J. J., Bargmann, C. I., Ahrens, M. B., Schreiter, E. R., Jayaraman, V., Looger, L. L., Svoboda, K.Kim, D. S., 2016. Sensitive red protein calcium indicators for imaging neural activity. eLife. 5.

Daviaud, N., Garbayo, E., Sindji, L., Martinez-Serrano, A., Schiller, P. C.Montero-Menei, C. N., 2015. Survival, differentiation, and neuroprotective mechanisms of human stem cells complexed with neurotrophin-3-releasing pharmacologically active microcarriers in an ex vivo model of Parkinson's disease. Stem cells translational medicine. 4, 670-84.

Elkabetz, Y., Panagiotakos, G., Al Shamy, G., Socci, N. D., Tabar, V.Studer, L., 2008. Human ES cell-derived neural rosettes reveal a functionally distinct early neural stem cell stage. Genes & development. 22, 152-65.

Erdei, Z., Lorincz, R., Szebenyi, K., Pentek, A., Varga, N., Liko, I., Varady, G., Szakacs, G., Orban, T. I., Sarkadi, B.Apati, A., 2014. Expression pattern of the human ABC transporters in

pluripotent embryonic stem cells and in their derivatives. Cytometry. Part B, Clinical cytometry. 86, 299-310.

Eriksson, P. S., Perfilieva, E., Bjork-Eriksson, T., Alborn, A. M., Nordborg, C., Peterson, D. A.Gage, F. H., 1998. Neurogenesis in the adult human hippocampus. Nature medicine. 4, 1313-7.

Ernst, A. and Frisen, J., 2015. Adult neurogenesis in humans- common and unique traits in mammals. PLoS biology. 13, e1002045.

Forostyak, O., Romanyuk, N., Verkhratsky, A., Sykova, E.Dayanithi, G., 2013. Plasticity of calcium signaling cascades in human embryonic stem cell-derived neural precursors. Stem cells and development. 22, 1506-21.

Gage, F. H. and Temple, S., 2013. Neural stem cells: generating and regenerating the brain. Neuron. 80, 588-601.

Guo, Q., Zhou, J., Feng, Q., Lin, R., Gong, H., Luo, Q., Zeng, S., Luo, M.Fu, L., 2015. Multi-channel fiber photometry for population neuronal activity recording. Biomedical optics express. 6, 3919-31.

Hagihara, H., Takao, K., Walton, N. M., Matsumoto, M.Miyakawa, T., 2013. Immature dentate gyrus: an endophenotype of neuropsychiatric disorders. Neural plasticity. 2013, 318596.

Hiragi, T., Andoh, M., Araki, T., Shirakawa, T., Ono, T., Koyama, R.Ikegaya, Y., 2017. Differentiation of Human Induced Pluripotent Stem Cell (hiPSC)-Derived Neurons in Mouse Hippocampal Slice Cultures. Frontiers in cellular neuroscience. 11, 143.

Jessberger, S., Zhao, C., Toni, N., Clemenson, G. D., Jr., Li, Y.Gage, F. H., 2007. Seizure-associated, aberrant neurogenesis in adult rats characterized with retrovirus-mediated cell labeling. The Journal of neuroscience : the official journal of the Society for Neuroscience. 27, 9400-7.

Kim, Y. S. and Park, C. H., 2011. Dopamine neuron generation from human embryonic stem cells. International journal of stem cells. 4, 85-7.

Koch, P., Opitz, T., Steinbeck, J. A., Ladewig, J.Brustle, O., 2009. A rosette-type, self-renewing human ES cell-derived neural stem cell with potential for in vitro instruction and synaptic integration. Proceedings of the National Academy of Sciences of the United States of America. 106, 3225-30.

Kohler, E. E., Cowan, C. E., Chatterjee, I., Malik, A. B.Wary, K. K., 2011. NANOG induction of fetal liver kinase-1 (FLK1) transcription regulates endothelial cell proliferation and angiogenesis. Blood. 117, 1761-9.

Kolacsek, O., Krizsik, V., Schamberger, A., Erdei, Z., Apati, A., Varady, G., Mates, L., Izsvak, Z., Ivics, Z., Sarkadi, B.Orban, T. I., 2011. Reliable transgene-independent method for determining Sleeping Beauty transposon copy numbers. Mobile DNA. 2, 5.

Kozubenko, N., Turnovcova, K., Kapcalova, M., Butenko, O., Anderova, M., Rusnakova, V., Kubista, M., Hampl, A., Jendelova, P.Sykova, E., 2010. Analysis of in vitro and in vivo characteristics of human embryonic stem cell-derived neural precursors. Cell transplantation. 19, 471-86.

Li, W., Sun, W., Zhang, Y., Wei, W., Ambasudhan, R., Xia, P., Talantova, M., Lin, T., Kim, J., Wang, X., Kim, W. R., Lipton, S. A., Zhang, K.Ding, S., 2011. Rapid induction and long-term self-renewal of primitive neural precursors from human embryonic stem cells by small molecule inhibitors. Proceedings of the National Academy of Sciences of the United States of America. 108, 8299-304.

Malmersjo, S., Liste, I., Dyachok, O., Tengholm, A., Arenas, E.Uhlen, P., 2010. Ca2+ and cAMP signaling in human embryonic stem cell-derived dopamine neurons. Stem cells and development. 19, 1355-64.

Malmersjo, S., Rebellato, P., Smedler, E., Planert, H., Kanatani, S., Liste, I., Nanou, E., Sunner, H., Abdelhady, S., Zhang, S., Andang, M., El Manira, A., Silberberg, G., Arenas, E.Uhlen, P., 2013. Neural progenitors organize in small-world networks to promote cell proliferation. Proceedings of the National Academy of Sciences of the United States of America. 110, E1524-32.

Marchetto, M. C., Carromeu, C., Acab, A., Yu, D., Yeo, G. W., Mu, Y., Chen, G., Gage, F. H.Muotri, A. R., 2010. A model for neural development and treatment of Rett syndrome using human induced pluripotent stem cells. Cell. 143, 527-39.

Mates, L., Chuah, M. K., Belay, E., Jerchow, B., Manoj, N., Acosta-Sanchez, A., Grzela, D. P., Schmitt, A., Becker, K., Matrai, J., Ma, L., Samara-Kuko, E., Gysemans, C., Pryputniewicz, D., Miskey, C., Fletcher, B., VandenDriessche, T., Ivics, Z.Izsvak, Z., 2009. Molecular evolution of a novel hyperactive Sleeping Beauty transposase enables robust stable gene transfer in vertebrates. Nature genetics. 41, 753-61.

Mateus-Pinheiro, A., Pinto, L., Bessa, J. M., Morais, M., Alves, N. D., Monteiro, S., Patricio, P., Almeida, O. F.Sousa, N., 2013. Sustained remission from depressive-like behavior depends on hippocampal neurogenesis. Translational psychiatry. 3, e210.

Mertens, J., Marchetto, M. C., Bardy, C.Gage, F. H., 2016. Evaluating cell reprogramming, differentiation and conversion technologies in neuroscience. Nat Rev Neurosci.

Mertens, J., Wang, Q. W., Kim, Y., Yu, D. X., Pham, S., Yang, B., Zheng, Y., Diffenderfer, K. E., Zhang, J., Soltani, S., Eames, T., Schafer, S. T., Boyer, L., Marchetto, M. C., Nurnberger, J. I., Calabrese, J. R., Odegaard, K. J., McCarthy, M. J., Zandi, P. P., Alda, M., Nievergelt, C. M., Mi, S., Brennand, K. J., Kelsoe, J. R., Gage, F. H.Yao, J., 2015. Differential responses to lithium in hyperexcitable neurons from patients with bipolar disorder. Nature. 527, 95-9.

Nicholas, C. R., Chen, J., Tang, Y., Southwell, D. G., Chalmers, N., Vogt, D., Arnold, C. M., Chen, Y. J., Stanley, E. G., Elefanty, A. G., Sasai, Y., Alvarez-Buylla, A., Rubenstein, J. L.Kriegstein, A. R., 2013. Functional maturation of hPSC-derived forebrain interneurons requires an extended timeline and mimics human neural development. Cell stem cell. 12, 573-86.

Orban, T. I., Apati, A., Nemeth, A., Varga, N., Krizsik, V., Schamberger, A., Szebenyi, K., Erdei, Z., Varady, G., Karaszi, E., Homolya, L., Nemet, K., Gocza, E., Miskey, C., Mates, L., Ivics, Z., Izsvak, Z.Sarkadi, B., 2009. Applying a "double-feature" promoter to identify cardiomyocytes differentiated from human embryonic stem cells following transposon-based gene delivery. Stem cells. 27, 1077-87.

Pentek, A., Paszty, K.Apati, A., 2016. Analysis of Intracellular Calcium Signaling in Human Embryonic Stem Cells. Methods in molecular biology. 1307, 141-7.

Reif, A., Fritzen, S., Finger, M., Strobel, A., Lauer, M., Schmitt, A.Lesch, K. P., 2006. Neural stem cell proliferation is decreased in schizophrenia, but not in depression. Molecular psychiatry. 11, 514-22.

Rose, T., Goltstein, P. M., Portugues, R.Griesbeck, O., 2014. Putting a finishing touch on GECIs. Frontiers in molecular neuroscience. 7, 88.

Sahay, A. and Hen, R., 2008. Hippocampal neurogenesis and depression. Novartis Foundation symposium. 289, 152-60; discussion 160-4, 193-5.

Shi, Y., Kirwan, P., Smith, J., Robinson, H. P.Livesey, F. J., 2012. Human cerebral cortex development from pluripotent stem cells to functional excitatory synapses. Nature neuroscience. 15, 477-86, S1.

Shin, R., Kobayashi, K., Hagihara, H., Kogan, J. H., Miyake, S., Tajinda, K., Walton, N. M., Gross, A. K., Heusner, C. L., Chen, Q., Tamura, K., Miyakawa, T.Matsumoto, M., 2013. The immature dentate gyrus represents a shared phenotype of mouse models of epilepsy and psychiatric disease. Bipolar disorders. 15, 405-21.

Smedler, E., Malmersjo, S.Uhlen, P., 2014. Network analysis of time-lapse microscopy recordings. Frontiers in neural circuits. 8, 111.

Steinbeck, J. A. and Studer, L., 2015. Moving stem cells to the clinic: potential and limitations for brain repair. Neuron. 86, 187-206.

Suzuki, I. K. and Vanderhaeghen, P., 2015. Is this a brain which I see before me? Modeling human neural development with pluripotent stem cells. Development. 142, 3138-50.

Tabar, V. and Studer, L., 2014. Pluripotent stem cells in regenerative medicine: challenges and recent progress. Nature reviews. Genetics. 15, 82-92.

Tamminga, C. A., Stan, A. D.Wagner, A. D., 2010. The hippocampal formation in schizophrenia. The American journal of psychiatry. 167, 1178-93.

Tatebayashi, Y., Lee, M. H., Li, L., Iqbal, K.Grundke-Iqbal, I., 2003. The dentate gyrus neurogenesis: a therapeutic target for Alzheimer's disease. Acta neuropathologica. 105, 225-32.

Toth, A. B., Shum, A. K.Prakriya, M., 2016. Regulation of neurogenesis by calcium signaling. Cell calcium. 59, 124-34.

Viero, C., Forostyak, O., Sykova, E.Dayanithi, G., 2014. Getting it right before transplantation: example of a stem cell model with regenerative potential for the CNS. Frontiers in cell and developmental biology. 2, 36.

Walton, N. M., Zhou, Y., Kogan, J. H., Shin, R., Webster, M., Gross, A. K., Heusner, C. L., Chen, Q., Miyake, S., Tajinda, K., Tamura, K., Miyakawa, T.Matsumoto, M., 2012. Detection of an immature dentate gyrus feature in human schizophrenia/bipolar patients. Translational psychiatry. 2, e135.

Yu, D. X., Di Giorgio, F. P., Yao, J., Marchetto, M. C., Brennand, K., Wright, R., Mei, A., McHenry, L., Lisuk, D., Grasmick, J. M., Silberman, P., Silberman, G., Jappelli, R.Gage, F. H., 2014. Modeling hippocampal neurogenesis using human pluripotent stem cells. Stem cell reports. 2, 295-310.

Zhao, C., Deng, W.Gage, F. H., 2008. Mechanisms and functional implications of adult neurogenesis. Cell. 132, 645-60.

Zhao, W. N., Cheng, C., Theriault, K. M., Sheridan, S. D., Tsai, L. H.Haggarty, S. J., 2012. A high-throughput screen for Wnt/beta-catenin signaling pathway modulators in human iPSC-derived neural progenitors. J Biomol Screen. 17, 1252-63.
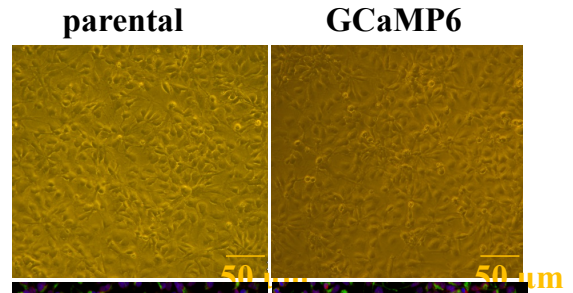
**Figures**

**Figure 1. Characterization of parental and GCaMP6-expressing NPCs and neurons**

(A) mRNA expression profiles of iPSC, parental and GCaMP6-expressing NPCs and neurons (at 4 weeks of differentiation), showing relative expression levels of key marker genes. (B-F) Investigation of the NPCs (B-C) and differentiated neurons (D-F) by immunocytochemistry. NPCs and neuronal cells were differentiated as described in Methods. NPCs and GCaMP6-expressing NPCs were transferred onto poly-ornihine/laminin coated eight-well chambers for confocal microscopy. The samples were fixed, permeabilized and stained with antibodies recognizing specific proteins for each cell type; Nestin (green) and SOX2 (red) for neural progenitors, MAP2 (red or gray), CALB1 (gray) and PROX1 (red) for neural cell types. Nuclei were counterstained with DAPI (blue).
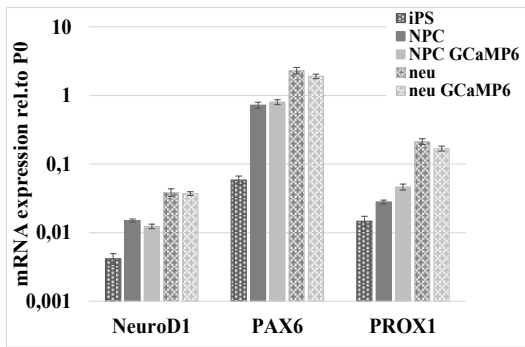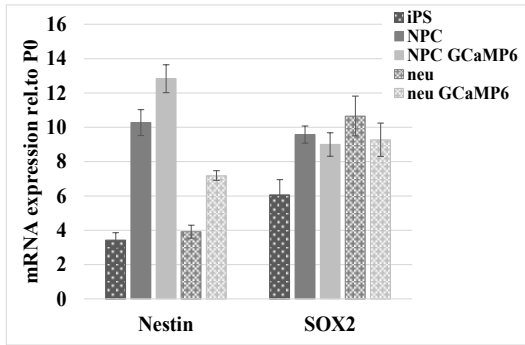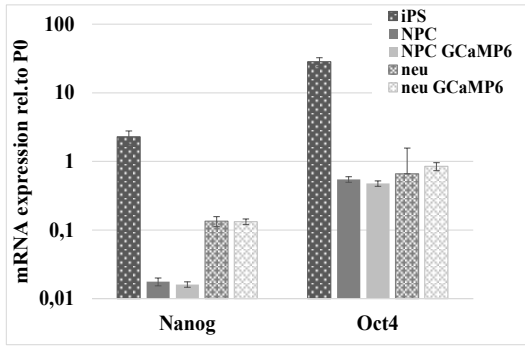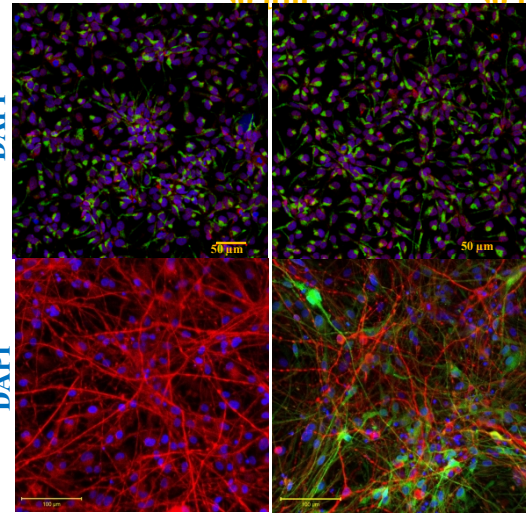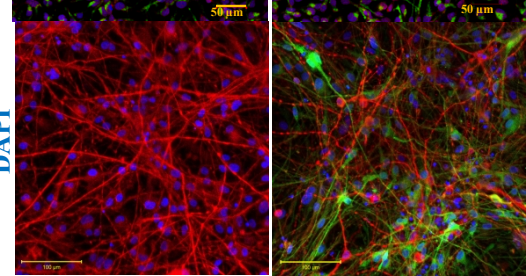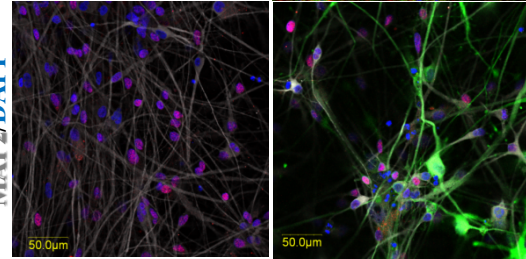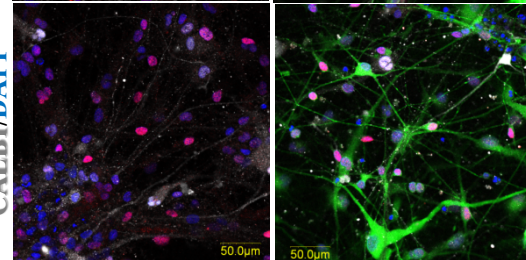
**Figure 2. Comparison of calcium signals in parental and GCaMP6-expressing NPCs.**

(A-B) Representative confocal microscopy images and calcium signals were measured in Fluo-4 loaded NPCs (A) or in GCaMP6-expressing NPCs (B). Mean values ± SD are presented on diagrams (A: n=200, B: n=129). Calcium signals were measured by confocal microscopy upon the addition of ATP (100 μM), LPA (10 μM), low concentrations of trypsin (2.5 μg/ml), and ionomycin (5 μM) - addition of the agents is indicated by the respective arrows. The maximum and minimum levels of the calcium-dependent cellular fluorescence were estimated in the presence of ionomycin, and after the addition of excess EGTA to the medium, respectively. The fluorescence data were normalized to a calibrated range of cellular calcium levels (Fmax–Fmin). (C-D) Effects of various signal inducing agents on responding cell numbers (C) and calcium signal intensities (D) are shown for Fluo-4 loaded and GCaMP6-expressing NPCs. Number of responding cells was calculated by determining the numbers of the cells that showed more than 10% elevation relative to basal calcium levels. Relative fluorescent intensities were calculated by determining maximal values after the indicated treatments, normalized to the calibrated range of cellular calcium levels (Fmax–Fmin), as described in panel A. Values represent the means ± SD of 3 independent experiments (ATP, LPA, TRY: Fluo-4: n1=265, n2=200, n3=181; GCaMP6: n1=82, n2=77, n3=129; GLUT: Fluo-4: n1=217, n2=139, n3=207; GCaMP6: n1=97, n2=113, n3=80). We found no significant difference between Fluo-4-loaded and GCaMP6-expressing cells in any case (two-sample t-tests, p>0.05). (E-F) Representative calcium signals of single cells demonstrating calcium oscillation after addition of ATP, LPA and trypsin for parental (E) and GCaMP6-expressing (F) NPC cells.
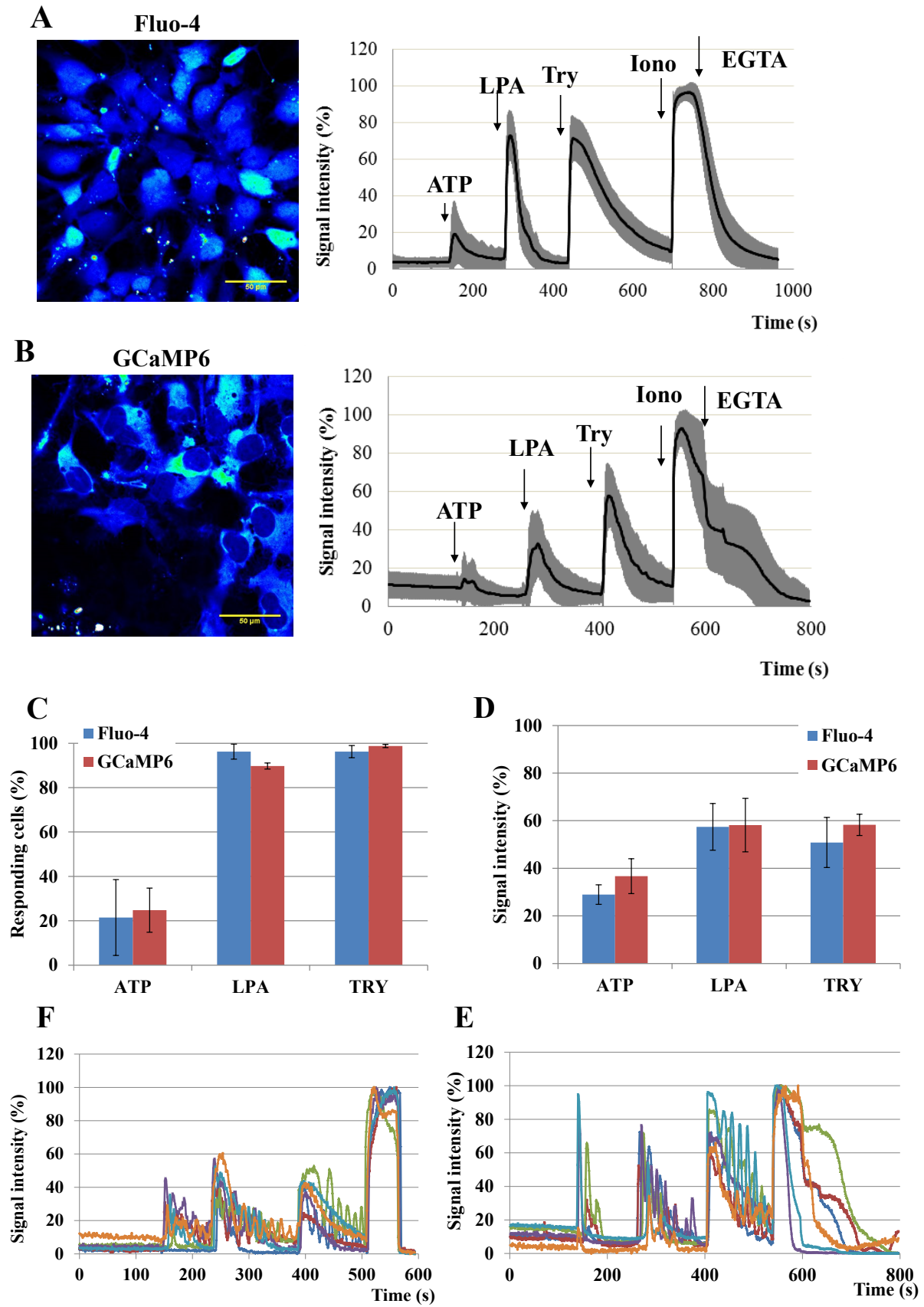
**Figure 3. Comparison of calcium signals in parental and GCaMP6-expressing neurons.**

(A-B) Representative confocal microscopy images and calcium signals were measured in Fluo-4 loaded neurons (A, n=110) or in GCaMP6-expressing neurons (B, n=109), black bold curves show the mean values. Calcium signals were measured by confocal microscopy upon the addition of 50 mM KCl, addition of the agent is indicated by the respective arrows.
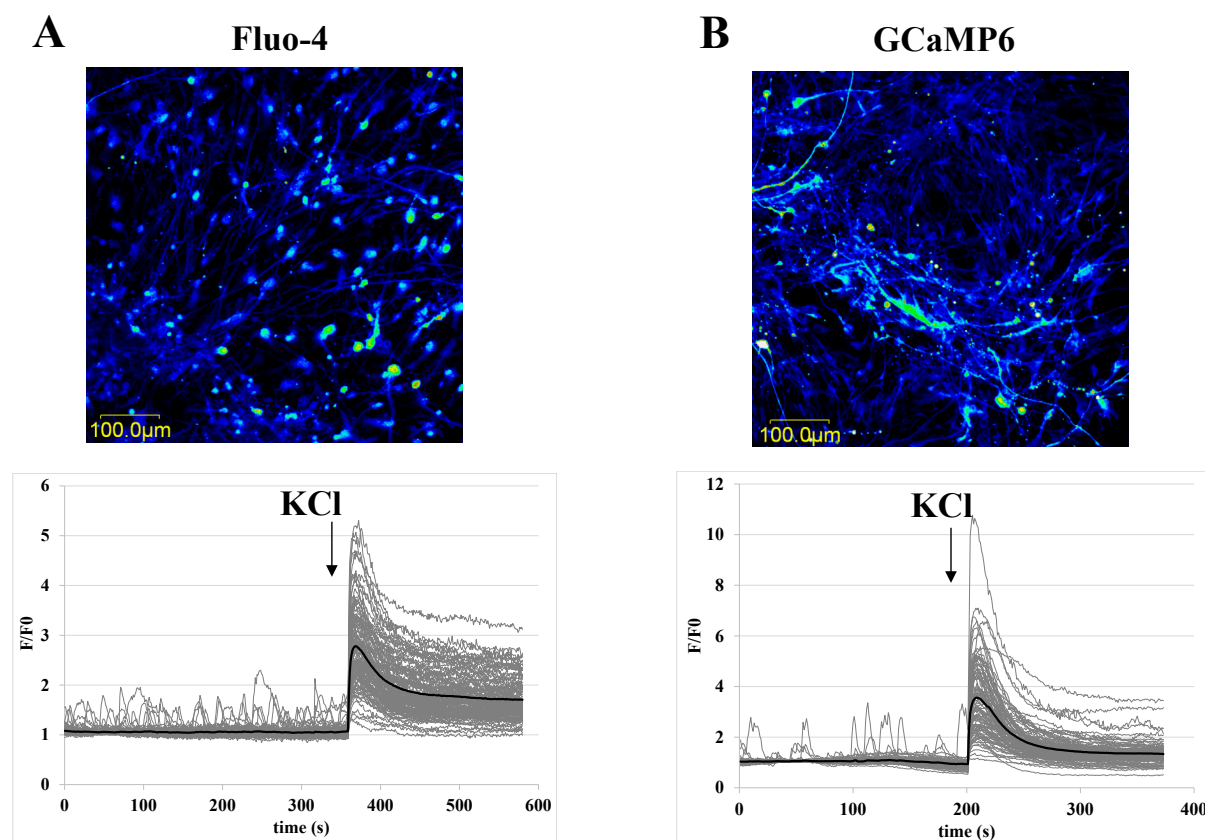


**Figure 4. Demonstration of spontaneous calcium transients in parental and GCaMP6-expressing neurons.**

Representative calcium signals of single cells (ROI 1-3) showing spontaneous calcium transients in neurons differentiated from parental and GCaMP6-expressing cells.



**Fluo-4 week old**



**GCaMP6-4 week old**



**GCaMP6- 10 days later**
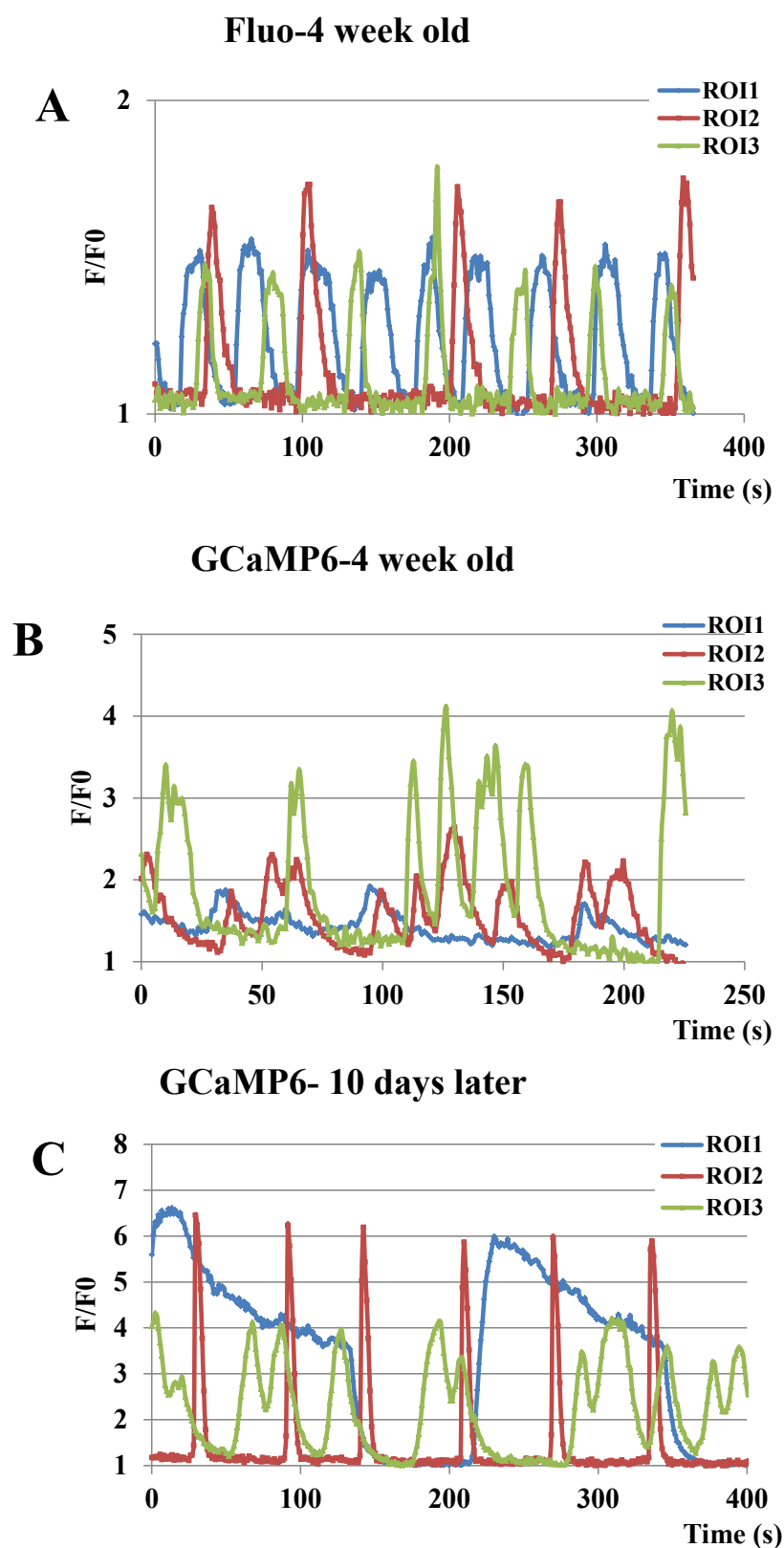
**Figure 5. Tetrodotoxin, an inhibitor of voltage-gated sodium-channels inhibits spontaneous activity both in parental (A, n=13) and GCaMP6-expressing neurons (B,**

27

**n=17).** TTX was administered at the concentration of 100 μM. Representative calcium signals of single cells showing spontaneous calcium transients in neurons differentiated from parental and GCaMP6-expressing cells. Black bold curves show the mean values.

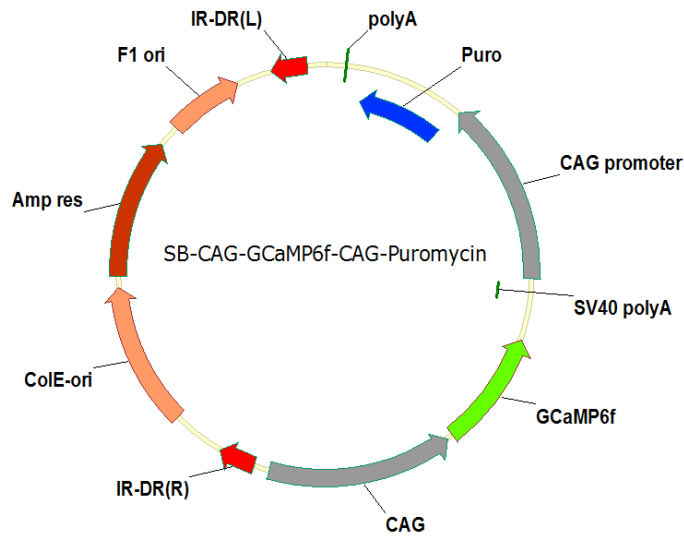**Fluo-4, 5 week old**



**GCaMP6, 5 week old**
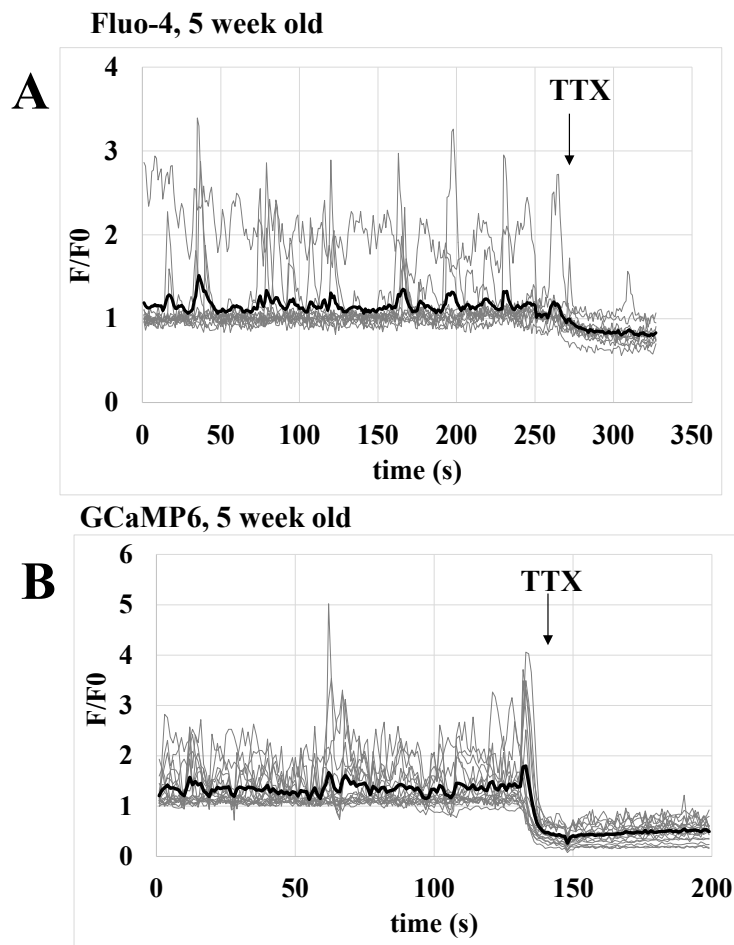
**Supplementary Figures**

**Supplementary Figure 1.**

(A) mRNA expression profile of spontaneously differentiated iPSC at day 3 and day 18, showing normalized expression levels of key marker genes (mesoderm-Brachyury, endoderm-AFP and ectoderm-Pax6). (B) Investigation of spontaneously differentiated iPSC at day 3 by immunocytochemistry (mesoderm-SMA, endoderm-AFP and ectoderm-B-III-Tubulin).
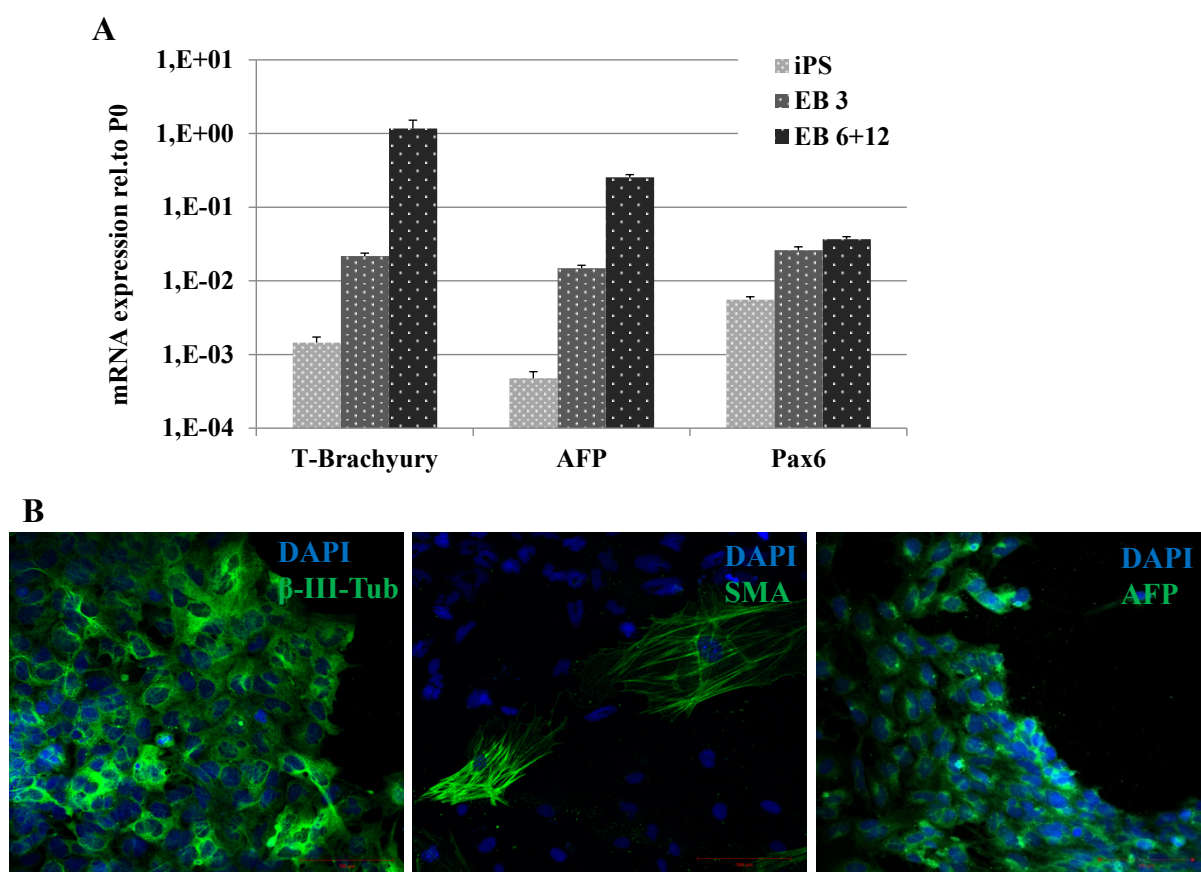


**Supplementary Figure 2.**

Vector construct scheme. Structure of the transfected plasmid for the *Sleeping Beauty* transposon system. IR-DR(L) and (R) stand for left and right inverted repeat-direct repeat transposon sequence, the GCaMP6fast and puromycin genes are driven by separate CAG promoters.

IR-DR(L)  polyA
F1 ori  Puro
Amp res  CAG promoter
SB-CAG-GCaMP6f-CAG-Puromycin
SV40 polyA
ColE-ori  GCaMP6f
IR-DR(R)  CAG

**Supplementary Figure 3.**

p values of mRNA studies presented on Fig 1 A,B and C.

**A**

| Oct4 / Nanog | iPS 62F | NPC 62F | NPC 62F | neu 62F | neu 62F GCaMP |
|---|---|---|---|---|---|
| iPS 62F | | 0.0004 | 0.0004 | 0.0004 | 0.0004 |
| NPC 62F | 0.0014 | | 0.1516 | 0.8382 | 0.0137 |
| NPC 62F GCaMP | 0.0014 | 0.3699 | | 0.7442 | 0.0061 |
| neu 62F | 0.0017 | 0.0009 | 0.0008 | | 0.7388 |
| neu 62F GCaMP | 0.0017 | 0.0001 | 0.0001 | 0.8929 | |

**B**

| Sox2 / Nestin | iPS 62F | NPC 62F | NPC 62F | neu 62F | neu 62F GCaMP |
|---|---|---|---|---|---|
| iPS 62F | | 0.0039 | 0.0104 | 0.0055 | 0.0135 |
| NPC 62F | 0.0002 | | 0.2989 | 0.2133 | 0.6534 |
| NPC 62F GCaMP | 0.0001 | 0.0163 | | 0.0993 | 0.7092 |
| neu 62F | 0.2164 | 0.0002 | 0.0001 | | 0.1887 |
| neu 62F GCaMP | 0.0002 | 0.0027 | 0.0003 | 0.0003 | |

**C**

| NeuroD1 / Prox1 / Pax6 | iPS 62F | NPC 62F | NPC 62F GCaMP | neu 62F | neu 62F GCaMP |
|---|---|---|---|---|---|
| iPS 62F | | 0.0001 | 0.0003 | 0.0003 | 0.0001 |
| NPC 62F | 0.0017 / 0.0001 | | 0.0216 | 0.0012 | 0.0001 |
| NPC 62F GCaMP | 0.0005 / 0.0001 | 0.0032 / 0.2418 | | 0.0008 | 0.0001 |
| neu 62F | 0.0001 / 0.0001 | 0.0001 / 0.0004 | 0.0002 / 0.0005 | | 0.6496 |
| neu 62F GCaMP | 0.0001 / 0.0001 | 0.0001 / 0.0002 | 0.0001 / 0.0003 | 0.0354 / 0.0655 | |

**Supplementary Figure 4.**

Representative calcium signals after addition of ATP (A, n=100, proportion of reactive cells: 9.0% for Fluo4 loaded and 8.0% for GCaMP6-expressing NPCs) and trypsin (C, n=100, proportion of reactive cells: 97.0% for Fluo4 loaded and 94.0% for GCaMP6-expressing NPCs) and the effect of specific inhibitors, suramin (a P2 purinergic receptor inhibitor, 600 µM) (B, n=150, no responding cells in either culture) and trypsin inhibitor (100 µg/ml) (D, n=150, no responding cells in either culture) respectively in Fluo-4 loaded and GCaMP6–expressing NPCs. The maximum and minimum levels of the calcium-dependent cellular fluorescence were estimated in the presence of ionomycin, and after the addition of excess EGTA to the medium, respectively. The fluorescence data were normalized to a calibrated range of cellular calcium levels (Fmax–Fmin).
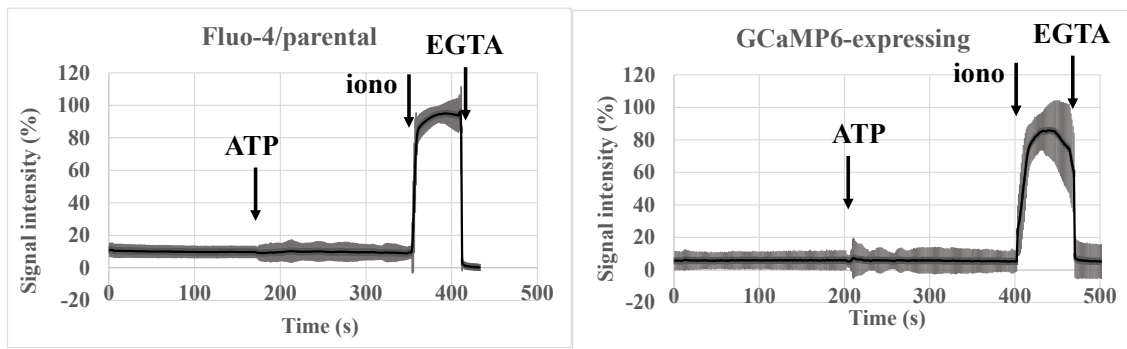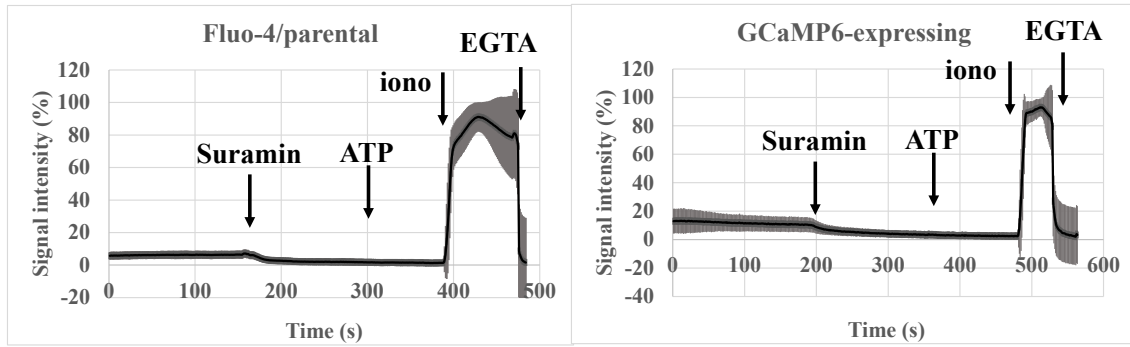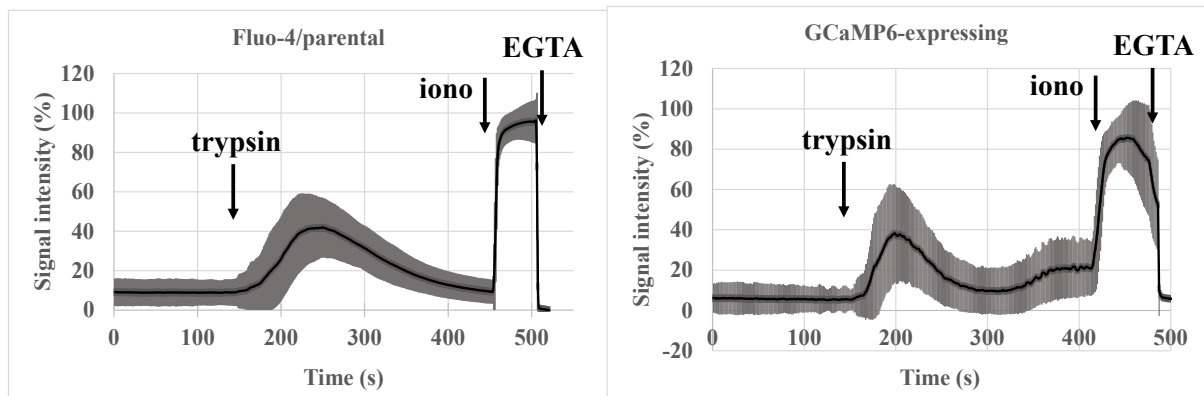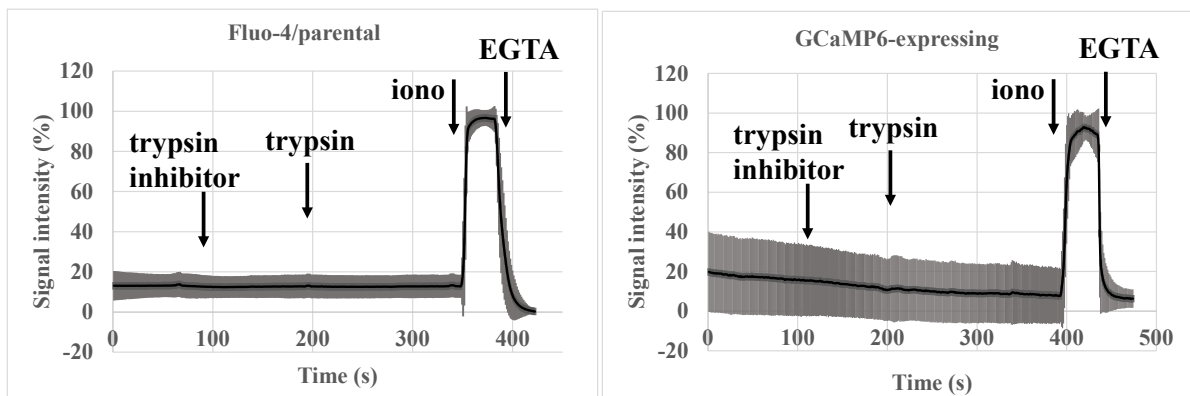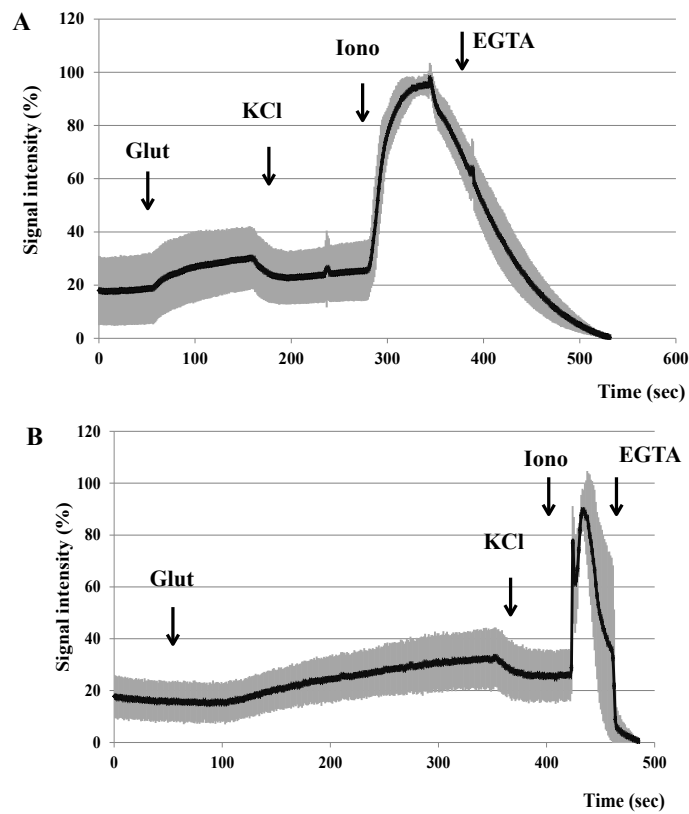
**Supplementary Figure 5.**

mRNA expression of GRIA1 (glutamate ionotropic receptor AMPA type subunit 1) at different passage numbers in parental and GCaMP6-expressing NPCs.
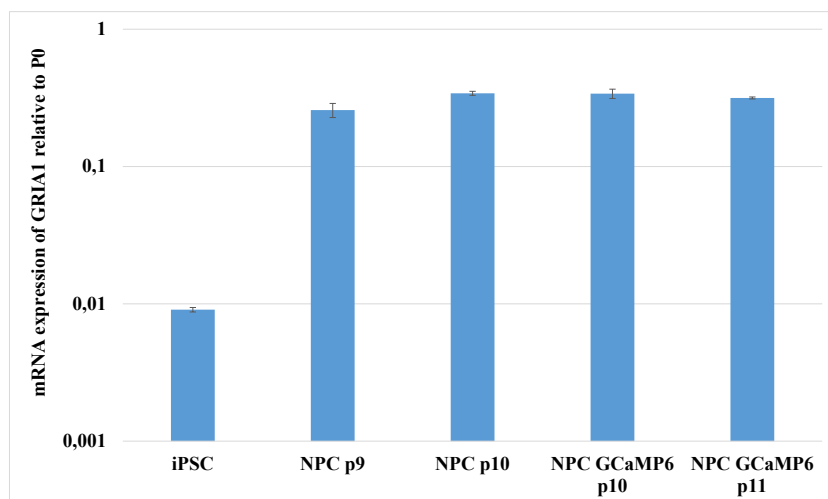


**Supplementary Figure 6.**

Representative calcium signals after addition of Glutamate, KCl, ionomycin and EGTA for Fluo4 loaded (A) and GCaMP6-expressing (B) NPCs. The maximum and minimum levels of the calcium-dependent cellular fluorescence were estimated in the presence of ionomycin, and after the addition of excess EGTA to the medium, respectively. The fluorescence data were normalized to a calibrated range of cellular calcium levels (Fmax–Fmin).

**Supplementary Figure 7.**

Effects of 50 µM Glutamate (A) or 50 mM KCl (B) on calcium signal intensities are shown for Fluo-4 and GCaMP6-expressing DG neurons. F/F0 values represent the means±S.E.M. of 3 independent experiments.

**A**

**B**
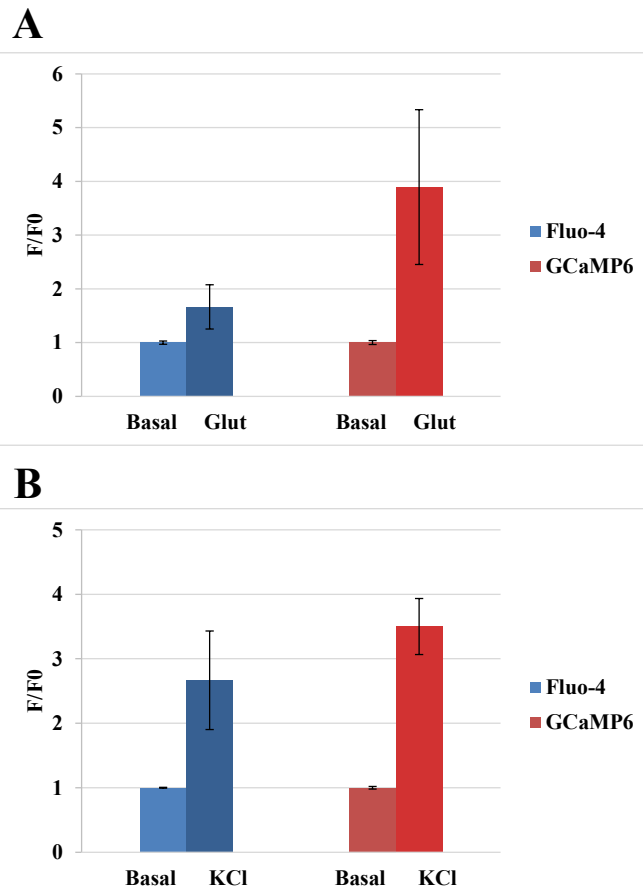
**Supplementary videos**

**Supplementary video 1.** Spontaneous calcium transients in GCaMP6-expressing neural cultures

The video shows spontaneous calcium signals in GCaMP6-expressing cells differentiated for 4 weeks on poly-ornithine/laminin coated confocal chambers.

**Supplementary video 2.** Spontaneous calcium transients in Fluo4 loaded neural cultures

The video shows spontaneous calcium signals in Fluo4 loaded cells differentiated for 4 weeks on poly-ornithine/laminin coated confocal chambers.